

Article

The Design and Testing of an Additive Manufacturing-Obtained Compliant Mechanism for the Complex Personalisation of Lenses in Clinical Optometry

Victor Constantin, Daniel Comeagă , Bogdan Grănescu * , Daniel Besnea and Edgar Moraru 

Department of Mechatronics and Precision Mechanics, Faculty of Mechanical Engineering and Mechatronics, National University of Science and Technology POLITEHNICA Bucharest, 060042 Bucharest, Romania

* Correspondence: bogdan.gramescu@upb.ro

Abstract: The precision needed in optometric measurements for the correct customization of progressive lenses usually falls short of what is required for accurate prescriptions. This usually stems from the fact that most measurements are obtained using outdated methods, employing either rulers or protractors. While there is equipment available for precise measurements, the cost of purchase and ownership is usually prohibitive. In this context, due to constant progress in high-resolution cameras along with the processing power of handheld devices, another solution has presented itself in different iterations in the past decade, as put forward by different manufacturers of optical lenses. Such a system comprises a mobile computing device with image capture and processing capabilities (tablet or smartphone), along with a marker support system to be mounted on the user's glasses frames. Aside from cost, the ease of implementation and usage, the advantage of such a system is that the parameters, as measured, allow for better customization, since the eyewear is already in the position in which it will be used. It allows the optometrist to measure parameters such as interpupillary distance, pantoscopic angle and the curvature of the eyewear in relation to the user's own specific shape and size. This paper proposes a model of a marker support system that is easy to use, precise, low in cost and has minimal impact on the measurements obtained by the optometrist. As such, this paper examines the steps for determining the shape needed for supports in relation to the measurements that need to be taken; a finite element analysis of the support was proposed, along with various tests and modifications that were made to the device until a specific shape and material combination was found that satisfied all of the parameters required. An experimental model of the system was produced and tested on a wide variety of glasses frames with good results, as presented in the following work.

Keywords: compliant mechanism; optometry; progressive lens customisation; additive manufacturing



Citation: Constantin, V.; Comeagă, D.; Grănescu, B.; Besnea, D.; Moraru, E. The Design and Testing of an Additive Manufacturing-Obtained Compliant Mechanism for the Complex Personalisation of Lenses in Clinical Optometry. *Appl. Sci.* **2023**, *13*, 13010. <https://doi.org/10.3390/app132413010>

Academic Editors: Florin Popișter, Sergiu Dan Stan, Nikola Vitković and Milan Banić

Received: 17 November 2023

Revised: 23 November 2023

Accepted: 27 November 2023

Published: 6 December 2023



Copyright: © 2023 by the authors. Licensee MDPI, Basel, Switzerland. This article is an open access article distributed under the terms and conditions of the Creative Commons Attribution (CC BY) license (<https://creativecommons.org/licenses/by/4.0/>).

1. Introduction

A model for a compliant mechanism to be used in the structure of a marker support system was developed and tested by various methods [1], with a final result being obtained in the form of the shape in Figure 1. The model took into account a force of 35 N maximum to be applied to each side of the marker support system, with PLA being used as a material to build the part by using Fusion Deposition Methods—thus obtaining a total stroke of approximately 30 mm, allowing for eyewear with a total height of up to 60 mm to be measured.

The first applications of additive manufacturing (AM) technologies in medicine date back to the end of the 20th century and refer to achievements in dental prosthetics and implantology [2,3]. Since then, these manufacturing methods have greatly developed, have exponentially progressed and are applied in almost all branches of the medical field, opening new horizons for mankind and improving the quality of life [4]. Nowadays, there are many uses of 3D printing for various complex prosthetic constructions applied in the dental field, or other types of orthopaedic prostheses [5–7], and these uses include making

models and prototypes for educational purposes [8], preparing/planning operations [9], creating surgical instruments [10] and other personalized medical tools that are anatomically suitable for each patient, applications in the field of pharmacology research [11] and even the creation of living tissues or cells [12].

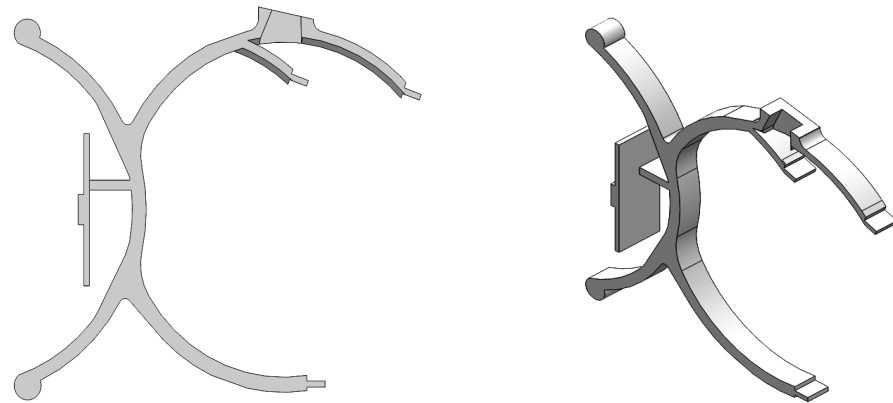


Figure 1. Front and isometric views of the model used for lateral marker support.

There have been recent evolutions in the optical and optometric fields, and the new applications of additive technologies have been felt [13,14]. For example, the appearance of personalized glasses frames obtained using additive technologies [15] can be considered a beginning for the further development and revolutionizing of the optometric field, respecting all the physiological and anatomical features of a person and taking into account the client's desires and his anthropometric data. Selective laser deposition technology [16,17] using metal/polymeric powders has proven to be the most suitable for the manufacturing of frames, and its advantage is the almost complete absence of scraps, unlike traditional production where considerable material losses are recorded. Additive technologies can also allow for the production of various lenses [18] and innovative and multifunctional components, which can simplify, optimize and miniaturize optical systems, being able to perfect medical instruments, equipment for scientific research or household equipment. It is also worth mentioning the efforts and special progress made in the ophthalmological field, using bioprinting for corneal reconstruction and regeneration or the creation of other eye tissues such as retina or conjunctiva [19–21]. Such research is in the advanced testing/research phase and has great prospects for use in the field in the future, bringing important contributions to the development of this medical area and major benefits for people with ocular disabilities.

Therefore, surely 3D printing will radically change the activity of an ophthalmologist, optician or optometrist for the better. The application described in this paper can fall into the category of assistive systems for optometric applications, and, as a basis for realization, utilized thermoplastic extrusion technology—FDM (fused deposition modelling) [1,22].

This paper demonstrates the steps that were taken in the design, preliminary finite element analysis, fabrication and testing of a novel shape and model of a marker support system for evaluating the measurements needed for obtaining specific parameters in the customisation of progressive lenses. The model was designed using flexible parts that would allow the position of markers mounted on the system to be influenced by specific parameters in a glasses' frame, as well as the relative position of the frame to the patient. The marker support system was 3D modelled and simulated with good results, which prompted the manufacturing of the system using FDM technology. Following initial tests, the support system was employed to test for specific parameters with good results in simple, preliminary trials.

2. Complete System Description

Shapes and materials previously studied [1] were used to create and assemble the system as presented in Figure 2a,b. The first of the two shows a frontal view of the marker

support system, as viewed by the optometrist. It comprises two compliant mechanisms: (1), one for each of the two openings of the glasses frames on which the system will sit by means of supports (2), (3) and (4). A large number of supports is needed to accommodate a large number of the shapes and sizes of glasses frames. As such, the mounting of the device onto a pair of glasses is performed by applying a force of up to 30 N to each side of the frame using handles (8), resulting in a larger opening between supports (2) and (4), as well as (2) and (3). Next, supports (3) and (4) are placed on the upper side of the frame, (2) is placed on the lower side and the force is removed. The bridge between the two lateral compliant mechanisms is flexible, allowing the support to match the glasses frame's curvature. The bridge comprises a central fixed section (6), a flexible portion (5) and a fixed marker support section (7). Lateral marker support is offered by means of support (9).

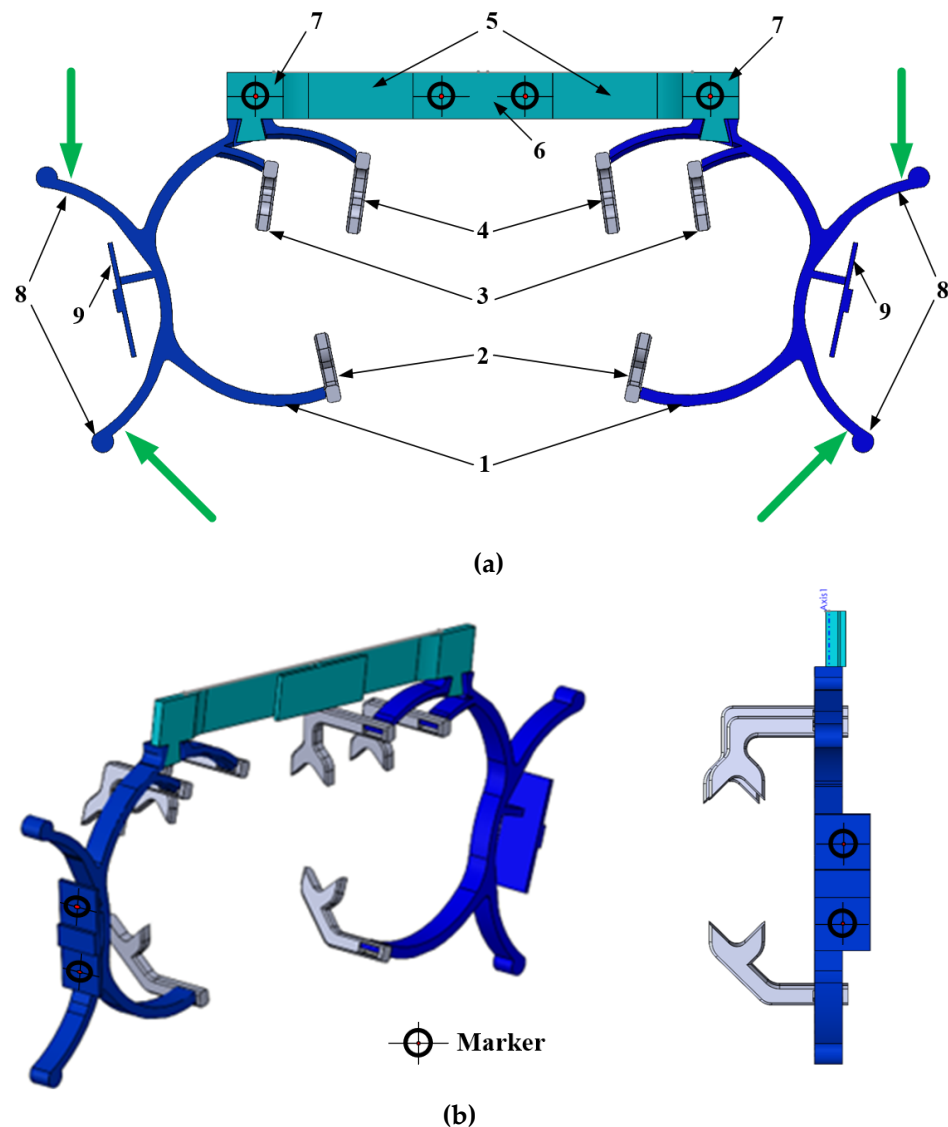


Figure 2. Views of the complete optometric model used for lateral marker support: (a)—front view; (b)—isometric and lateral views.

The device is built in modules to both allow, in some instances, for different materials to be used and improve on some of the parameters of the final product. Printing three separate parts allows for better quality, lower print times and a wider range of desktop printers that might be used to manufacture the device.

Regarding the movement of the markers due to the deformation of the device, both the lateral (side) markers and the central ones are mounted on small, single cantilever plates

that are not deformed during the mounting process. The distance between these points is known (calibrated) and serves as a reference during the measurements. The idea of directly printing the colour markers was certainly considered; issues with material colour consistency convinced us to use conventionally printed colour markers.

The support is used to position a set of markers relative to a user's face and determine, using a method to be discussed in another paper, dimensions specific to the user's facial parameters and chosen glasses frames. It allows for the acquisition of parameters such as the following: pupillary and interpupillary distance, curvature of the glasses frames, pantoscopic angle on both sides of the user's face as well as measurements related to customizing the lens to the glasses frames. The markers used are manufactured on adhesive, low-gloss paper of a specific colour and are positioned using a specially made stencil in order to guarantee their position. Figure 3 shows a chart of the measurements that can be taken using this system. This system allows all necessary parameters to be determined by taking both a close-up and a far picture of the patient wearing the glasses and marker support assembly.

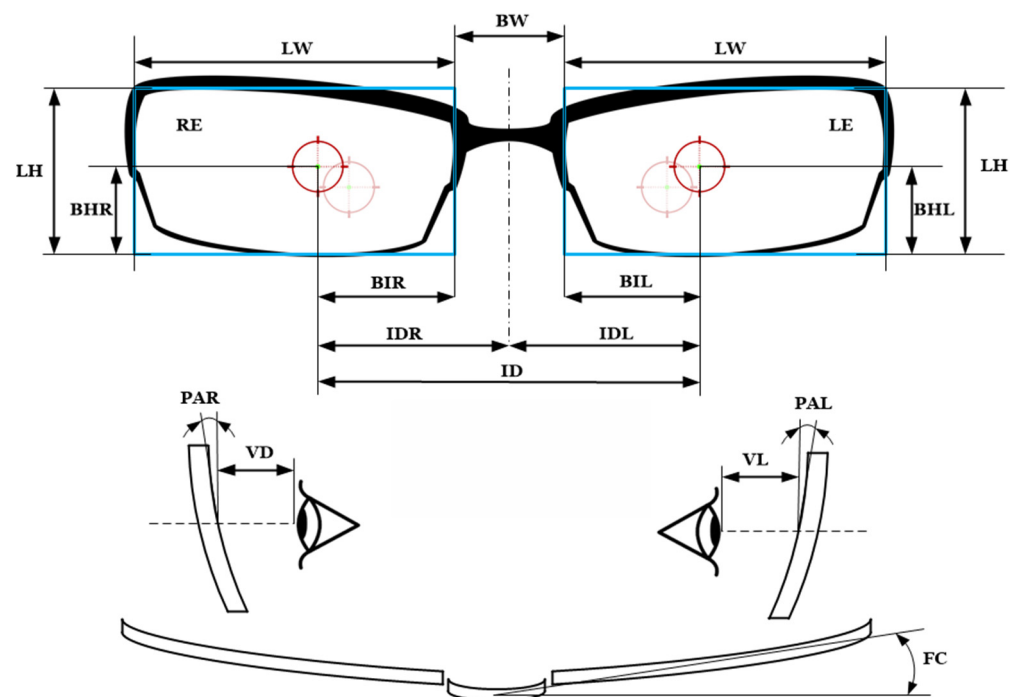


Figure 3. Measurements taken by the system.

Among the measurements that can be taken are the following: IDR (interpupillary distance, total as well as right IDR and left IDL), LW (lens width, both left and right), LH (lens height, left and right), BW (Bridge Width), BHR and BHL (pupil distance to lower part of lens) as well as BIL and BIR (pupil distance to lower part of lens). Along these, measurements related to vertex distance (VL and VD), distance between the pupil and lens, PAR and PAL (left and right pantoscopic angle) as well as the glasses frame curvature FC are included.

3. General Estimation of the Assembly's Mechanical Behaviour before Manufacturing

This chapter is centred on analysing the mechanical behaviour of the proposed structure, using specific numerical engineering simulation tools and the finite element method [1,23]. Currently, finite element simulations are powerful analysis instruments that have a deep theoretical basis in the solving of a wide range of technical problems [24–33], not least in the biomedical field [34,35] and including the ophthalmology/optometric field [1,36], to improve medical devices before their realization. Considering the nature of the physical and mechanical properties of the thermoplastic materials used for the FDM

process, but also due to the specific peculiarities of the layered structure that make it difficult to establish a simulated numerical solution as close to reality as possible, the aim of this study is to approximate the behaviour of the structure, according to applied loads during operation, on a given type of glasses before the manufacturing of the system and to obtain preliminary results and an estimate of the displacement of the marker support system. For this purpose, a structural static type of analysis was used, and polylactic acid (PLA) was chosen as the base material in the simulation—the properties attributed to the material being the same as in the previous authors' paper [1]—with Young's modulus established experimentally [37,38].

The following paragraphs will present the stages and results obtained from the simulation of the structure of the complete compliant mechanism proposed, using the FEA method, as well as the mechanical loads that occur during its operation, using the Solid Works program. The following classical steps regarding FEA simulation were applied: designing and modelling the structure, creating the mathematical model and physical conditions—choosing the multiphysics module, assigning the material, establishing fixed geometries, assigning the loads, dividing the loads into finite elements and running and interpreting the results.

The central element of the bridge was established as fixed geometry, and mechanical loads were established as input data; a normal force of 15 N was applied to the four faces of the grasping structure, according to the loads proposed from a previous paper [1]. Additionally, torques of the absolute value of 0.002 N·m, with opposite signs around an imaginary vertical axis on the lateral faces of the bridge, were applied.

Figure 4 presents the results obtained from the FEA simulation of the complete structure proposed for the optometric application, regarding the resultant displacement on all three axes and equivalent von Mises stress. It is possible to observe how the highest values intervene in the inferior area of the grasping elements with the maximum resultant displacement value of 39.39 mm. Regarding the equivalent von Mises stresses, the most affected regions appear at the flexible part of the bridge but also appear in some areas of the grasping element, with all values nevertheless being below the yield strength of the material for the loads applied, validating the model proposed.

In Figure 5a, it is possible to notice the displacements obtained on the vertical axis (Z), i.e., the maximum openings of the mechanism resulting from the loads applied. These are values of interest, because they indicate the size of the eyeglasses on which the mechanism can operate. For example, the maximum and minimum values can be identified on the figure, i.e., the maximum displacements from the initial position of hypothetical contact surfaces with eyeglasses (11.653 mm and -1.387 mm, respectively). Summing up their absolute values, an opening of 13.04 mm can be obtained from the initial distance between the grasping elements (namely contact surfaces with eyeglasses); therefore, in the case of simulation with the proposed material and applied loads mentioned above, this mechanism is able to operate on eyeglasses with a size greater than 13 mm, compared to the initial design distance of the grasping elements of the compliant mechanism (falls within the range of eyeglasses size with which the proposed mechanism can operate). In Figure 5b, some details regarding the results of the displacement on the Y axis can be identified, following the torque applied in the area of the lateral part of the bridge, where maximum values of over 10 mm are obtained. Figure 5c illustrates the results of the movement on the Z-axis—only for the grasping elements where the maximum values, minimum values and distribution of displacements can only be seen in the mentioned areas of interest. In all of the cases in Figure 5, the initial positions of the entities of the structure are highlighted.

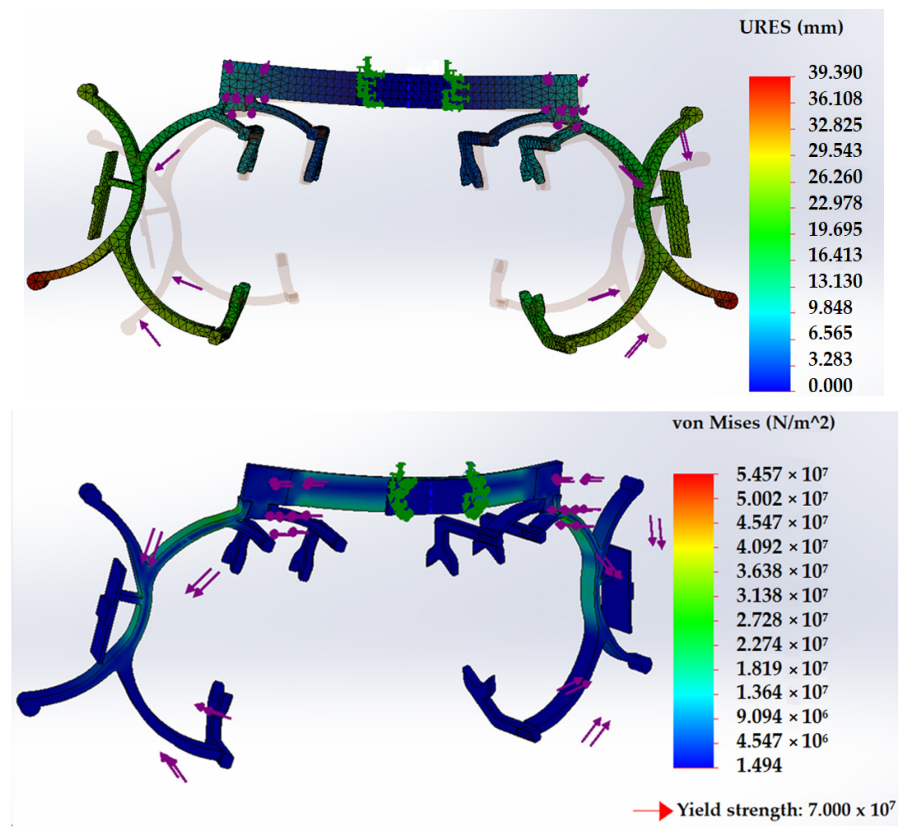


Figure 4. Obtained displacements (resultant displacement) and von Mises stress results for the compliant mechanism.

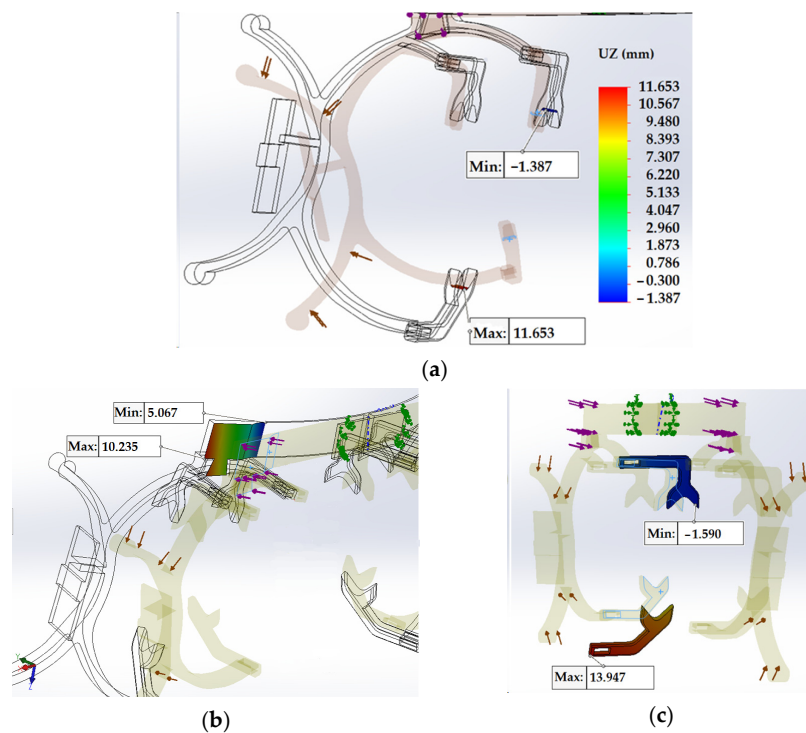


Figure 5. Some details of the results obtained after a FEA estimation of the structure proposed: (a)—Resulting opening of the mechanism (vertical Z axis) at 13.04 mm after load application; (b)—Y axis displacement of the lateral part of the bridge; (c)—Z axis displacement of the grasping elements.

Figure 6 presents an image depicting the simulation of the compliant mechanism's operation; in this, it is possible to observe the grasping of a certain type of eyeglasses, thereby validating the complete system model of the compliant mechanism proposed and being able to proceed with its realization and testing.

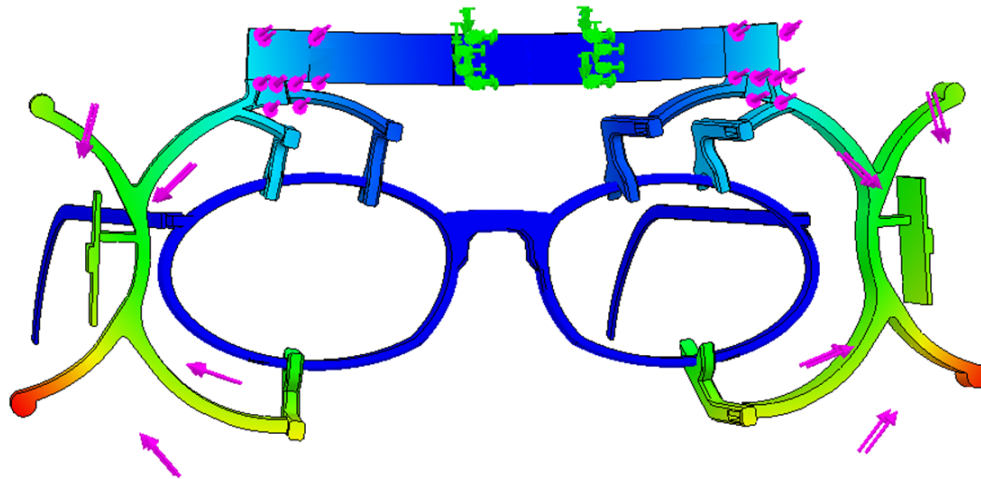


Figure 6. A simulation of the operation of the compliant mechanism proposed for the optometric field.

4. Manufacturing of a Prototype and Preliminary System Testing

Current additive manufacturing technologies allow for complex mechanisms to be tested before mass production—however, in some instances, they even allow for direct-to-customer-use manufacturing. For our designed mechanism, such a path was chosen, in that small batches could be produced and modified for specific needs in terms of the shapes of glasses frames. It is also important to note here that the current wide array of both materials, as well as composites, allow for the mechanism to be customized even further in terms of mechanical properties, look and feel, while taking into consideration that almost all of the changes to the material will, in some capacity, modify the way the mechanism transmits force and motion through elastic body transformation.

To this end, several materials were considered, of course, principally taking into consideration the notion that they should be inherently chemically inert to external use with the person wearing the glasses and the support system. Using this as a starting point and after some tests and consideration, as presented in a previous study [1], a specific version of thermoplastic polyurethane was chosen [1], with some of the material's properties being density 1.18 g/cm^3 , a Young modulus of 0.396 GPa and a yield strength of 65.85 MPa . While these parameters are specific to this material and do allow for the imposed travel of the mechanism's supports at approximately 30 mm at a 35 N -applied force on each end, further research has proven that such mechanical behaviour can also be obtained by using other materials, such as specific variants of Polylactic acid PLA. Also, some studies could be performed in order to determine to what extent, for this specific shape and purpose, slicing and FDM [37–42] parameters influence compliant behaviour, as well as long term use of the system.

Regarding FDM parameters, while a general-purpose FDM slicing software was used, specific parameters were tested in order to allow for the best results, both cosmetic and structural. Regarding the actual additive manufacturing system, a general-purpose desktop cartesian system was used, Prusa i3 model, capable of temperatures that are compatible with working with materials such as TPU or Nylon. It should be noted here that, since the material is flexible, a direct drive extruder is needed, with adjustments made to the pretensioning mechanism, specific to the elasticity of the material used. As for some of the specific parameters used during slicing, a low speed was selected (20 mm/s) for the infill, with an even lower speed of 15 mm/s for the outer walls. Infill was selected as full (100%), with a wall thickness of 0.8 mm , with bottom and top walls at a minimum of 1.2 mm . During

several tests performed, it was concluded that, in order to obtain the best results in both elasticity and overall mechanism usability, an infill of 100% should be used. There was also no advantage to be had by experimenting with other infill percentages since, with these current parameters, all of the requirements, such as shape and weight, were met.

The physical model was tested on a wide array of shapes of glasses, with a height from approximately 27 mm up to 60 mm, with good results in terms of both ease in fixing the support and maintaining its position in use. The model was proven to allow for accurate measurements of previously specified parameters (see Figure 3). Also, the model proved to allow for movement on behalf of the patient, without disturbing the position of the device once it was fixed to the frames.

During the tests, it was determined that, while certain rarer models of frames might pose an issue—such as extremely large or small models, as the ones encountered in use for children—the model could be easily modified to fit such situations. In some cases, this can be done by simply removing the supports used to fix the device to the frames. Figure 7a–c shows the support mounted on different shapes of glasses, as empirically determined to be among the most chosen by users.

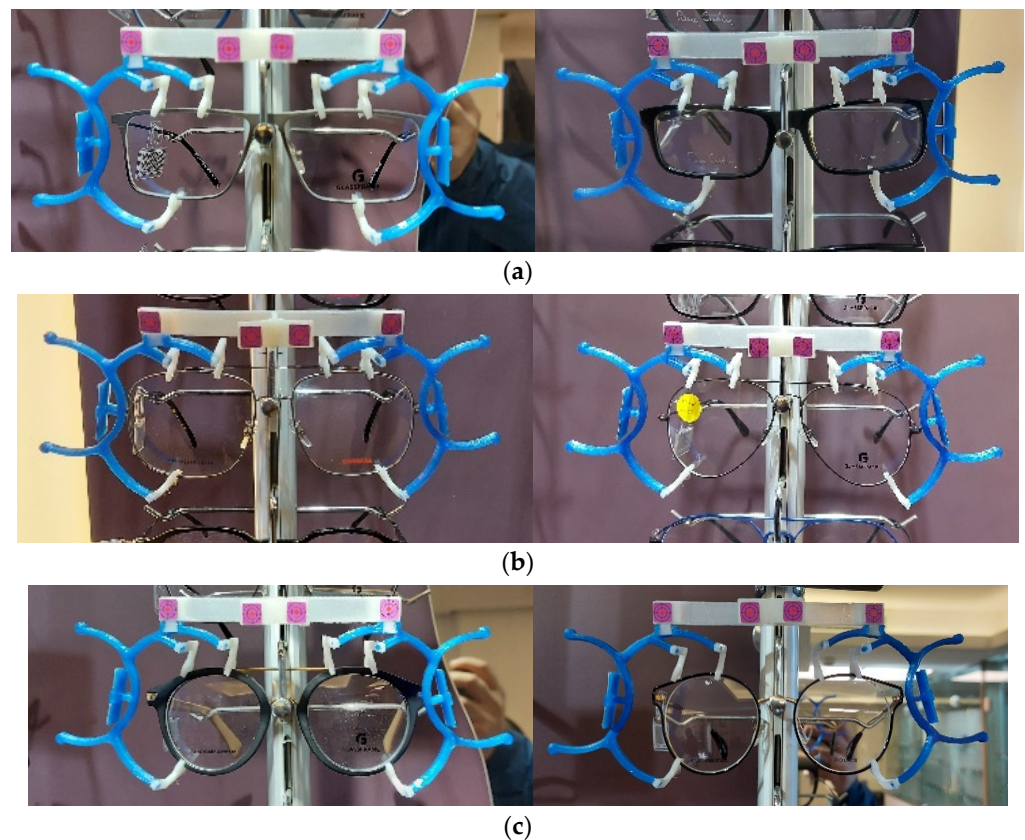
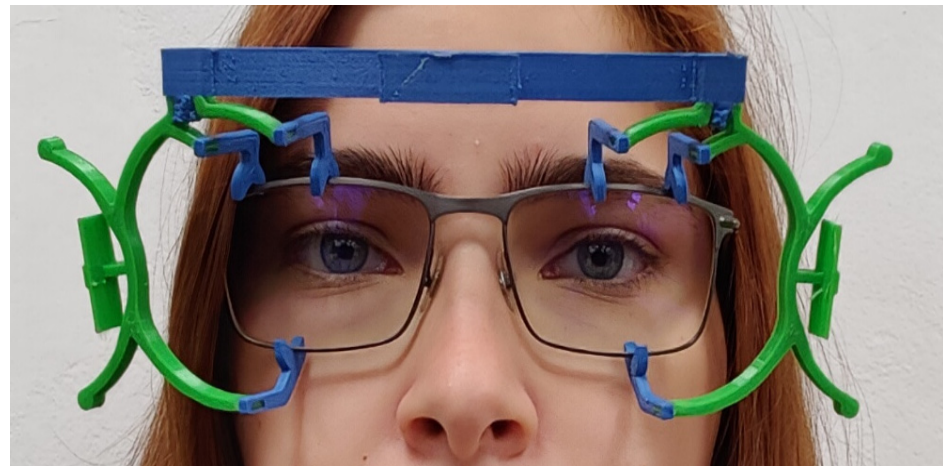


Figure 7. (a) “Regular”-shaped glasses frames. (b) Large glasses frames in terms of both width and height. (c) Round-shaped glasses frames.

Given the good results obtained in testing the marker support system for almost all pairs of glasses tested—with the exception of extremely small or overly large frames, with heights either under 25 mm or above 65 mm—it was concluded that tests could be performed with an actual patient to determine how wearing the supports would influence the measurements taken. While preliminary tests could be performed without a human subject, some parameters could not be simulated—for example, the user might wear the glasses slightly tilted to one side, or certain asymmetries might influence the position of the marker support system in such a way that measurements might be harder to obtain. For this purpose, a human test subject was involved in further investigation, as described in Section 5.

5. Evaluation of the Compliant Mechanism on a Human Patient

In order to confirm that the designed frame would indeed hold its shape when worn by a user and allow for the system to capture certain parameters, tests were performed that involved the device being fixed to a user's glasses, and information was obtained via visual, then computerized, confirmation that the user's parameters were indeed similar to those measured by other means. Such an example is shown in Figure 8a–c, discussed in detail as follows.



(a)



(b)



(c)

Figure 8. (a) Front view of the patient wearing test glasses and the marker support system. (b) Lateral view of the patient wearing the glasses and the marker support system. (c) Upper view of the glasses with the marker support system.

Figure 8a exhibits a user wearing a “regular” type of glasses frames, along with the marker support system. As can be observed, the supports are not, in any way, inconvenient to the user and allow the optometrist to easily monitor the user’s eyes in order to easily monitor for different conditions, such as the squinting that might only occur during specific actions taken by the patient. Since the marker’s weight is under 12 g, its effect on the angle of the glasses frames that is relative to the patient is minimal and can be neglected.

Figure 8b allows for a view of the patient wearing the supports along with the glasses frames. This view also allows for confirmation that the markers will, at least visually (to be later confirmed by image processing), allow for an approximation of the user’s pantoscopic angle. While it is usual to take only one pantoscopic angle into consideration, the system was designed to allow for different measurements to be taken both for the user’s left-side and right-side pantoscopic angle. This view also confirms that, due to the offset of the support system relative to the glasses frames, there is no interaction between the user and the compliant mechanism.

Figure 8c consists of a top-down view of the glasses and compliant mechanism, allowing for confirmation that the curvature of the frames is indeed transferred to the measuring system. Due to the very low force needed to bend the bridge between the two C-shaped main supports, the influence of the marker support system on the curvature of the glasses can be considered non-existent.

As such, it was indeed confirmed that the device mimics the user’s pantoscopic angle and the frame’s curvature, allowing for an easy measurement of the distance between the lens and the patient’s eyes, as well as simpler measurements, such as interpupillary distance, lens size, etc. The methods used to determine these parameters will be described in detail in further work and are the subject of a different side of the research that was undertaken in the creation of the system.

Overall, the mechanism was proven to be easy to use and appropriately sized when mounted on most pairs of glasses frames, with minimal or no effect on the position of the frames relative to the user’s face. Also, the support was easy to mount and was in no way inconvenient to the patient.

Using the images captured of the patient wearing the glasses mounted with the marker support system, several tests were conducted to confirm the validity of the assumptions made by the authors during the design process. As such, using a pre-alpha test application, also developed during the work done in this paper (preliminary results have indeed been found to confirm that the measurements taken are close to reality), was conducted by comparing image processing results with those obtained using the usual measurements. Figure 9 depicts the results obtained by analysing an image similar to that in Figure 8a, with markers added in their respective positions.

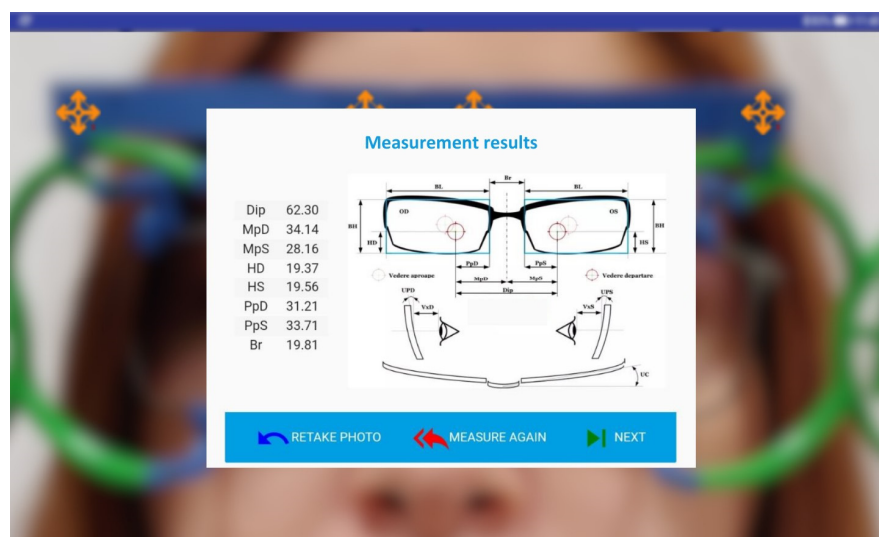


Figure 9. Results obtained during preliminary image recognition measurements.

6. Conclusions

Some of the harder-to-overcome obstacles encountered in the building of these prototypes were shape design, material choice and additive manufacturing techniques to be employed in the manufacturing of the compliant mechanism.

Regarding shape, the design can be split into two separate points to be addressed: one responsible for fixing the support to the frames as well as a bridge that would join the two C-shaped supports. While the initial design of the C-shaped supports was proposed and tested in previous works, adding a bridge introduced a number of issues previously not accounted for: rotation around the Y-axis of the frames, partially compensated by the shape of the joints between the bridge and supports, as well as a larger Y-axis dimension for the bridge, allowing for less rotational movement. The bridge, however, needed to be flexible enough to allow the entire system to follow the curvature of the frames.

The materials used were also scrutinized in terms of weight, ease of use, availability and, last but not least, compatibility with use in close proximity to human skin. While it might be argued that the support itself should not touch the patient at any time, it was considered necessary to guarantee that all the materials used were biologically inert to humans. That being said, while materials such as PLA or TPU, as used in this work, are commonly used around humans, a further scaling or usage of the system with different types of frames might prove to be necessary in order to explore other options.

Following these two choices, a preliminary FEM analysis was performed in order to estimate what could be expected of the mechanism without actually manufacturing it. General estimations performed during this stage were consistent with initial expected results, and this allowed the shape to be tweaked.

The additive technology used for the purposes of this work was FDM, but other candidates might also be considered, such as Digital Light Processing DLP or even Selective Laser Sintering SLS. While the obvious advantage of FDM is its accessibility, high-precision and more advanced materials might require different additive techniques to be used in order to obtain desired results in the mechanical behaviour of a device. There is also the concern of aesthetics—while FDM is precise enough to allow for usability, it is hardly the best in terms of surface quality.

Further work will be performed to design and perfect an application to be used alongside the marker support system in order to obtain measurements. This application will also allow for tests to be made that will further allow for possible modifications to be made to the shape of the part. This application will allow for a mobile computing and image capture device in order to use the markers mounted on the support for determining some parameters relevant to the construction of highly customised progressive lenses. Also, this application will allow for the user's details to be saved in a database and monitored over time, resulting in higher standards in healthcare. This application might even be connected to an online store and might allow users to directly customise their lenses after their measurements have been taken.

While the manufactured and tested marker support system has yielded good results, including in preliminary software tests not depicted in this paper, further extensive measurements need to be made using the system, and a full in-depth evaluation should be performed to assess the viability of the model proposed. There is also a valid point to be made for the pursuit, to a specific extent, of a parametric automated design for elastic elements in order for more shapes and sizes of frames to be measured.

The advantages of such a system stem from the fact that small changes can be made to the shapes so that all the models of the frames can be measured using this device. It is also understood that this system takes full advantage of the fact that FDM technologies have advanced and are regularly available in most areas of the world. Long-term, the gathering of measurement data through such a device would allow for certain approximations to be made by means of big data processing and, of course, including the results in the obtention of better and better measurements and more precise prescriptions for patients.

It is expected that this device will allow for more precise, cost-effective measurements to be taken in order to allow for a much better customisation of lenses in general, and progressive lenses in particular, ultimately allowing for better eye healthcare to be brought to a much wider range of patients.

Author Contributions: Conceptualization, V.C.; methodology, V.C., D.B. and B.G.; software, V.C.; validation, E.M., D.B. and D.C.; formal analysis, B.G., D.B. and D.C.; investigation, D.B. and V.C.; resources, B.G., D.B. and E.M.; writing—original draft preparation, V.C., E.M., D.C. and B.G.; writing—review and editing V.C., E.M., D.C. and B.G. All authors have read and agreed to the published version of the manuscript.

Funding: The publication of this paper was funded by the National University of Science and Technology Politehnica Bucharest’s PubART project.

Institutional Review Board Statement: Ethical review and approval were waived for this study through POLITEHNICA University of Bucharest Ethics Committee, due to no direct or indirect risk to the test subject as well as no specific rules and regulations for this type of study.

Informed Consent Statement: Informed consent was obtained from all subjects involved in the study. Written informed consent has been obtained from the patients to publish this paper.

Data Availability Statement: Data are contained within the article.

Conflicts of Interest: The authors declare no conflict of interest.

References

1. Constantin, V.; Besnea, D.; Gramescu, B.; Moraru, E. Aspects Related to the Design and Manufacturing of an Original and Innovative Marker Support System for Use in Clinical Optometry. *Appl. Sci.* **2023**, *13*, 2859. [\[CrossRef\]](#)
2. Liaw, C.Y.; Guvendiren, M. Current and emerging applications of 3D printing in medicine. *Biofabrication* **2017**, *9*, 024102. [\[CrossRef\]](#) [\[PubMed\]](#)
3. Dawood, A.; Marti, B.; Sauret-Jackson, V.M.; Darwood, A. 3D printing in dentistry. *Br. Dent. J.* **2015**, *219*, 521–529. [\[CrossRef\]](#)
4. Paul, G.M.; Rezaenia, A.; Wen, P.; Condoor, S.; Parkar, N.; King, W.; Korakianitis, T. Medical applications for 3D printing: Recent developments. *Mo. Med.* **2018**, *115*, 75. [\[PubMed\]](#)
5. Ginestra, P.; Ferraro, R.M.; Zohar-Hauber, K.; Abeni, A.; Giliani, S.; Ceretti, E. Selective laser melting and electron beam melting of Ti6Al4V for orthopedic applications: A comparative study on the applied building direction. *Materials* **2020**, *13*, 5584.
6. Vaish, A.; Vaish, R. 3D printing and its applications in Orthopedics. *J. Clin. Orthop. Trauma* **2018**, *9*, S74–S75. [\[CrossRef\]](#)
7. Ramakrishnan, T.; Schlafly, M.; Reed, K.B. Evaluation of 3D printed anatomically scalable transfemoral prosthetic knee. In Proceedings of the 2017 International Conference on Rehabilitation Robotics (ICORR), London, UK, 17–20 July 2017; IEEE: Piscataway, NJ, USA, 2017; pp. 1160–1164.
8. Garcia, J.; Yang, Z.; Mongrain, R.; Leask, R.L.; Lachapelle, K. 3D printing materials and their use in medical education: A review of current technology and trends for the future. *BMJ Simul. Technol. Enhanc. Learn.* **2018**, *4*, 27. [\[CrossRef\]](#)
9. Tejo-Otero, A.; Buj-Corral, I.; Fenollosa-Artés, F. 3D printing in medicine for preoperative surgical planning: A review. *Ann. Biomed. Eng.* **2020**, *48*, 536–555. [\[CrossRef\]](#)
10. George, M.; Aroom, K.R.; Hawes, H.G.; Gill, B.S.; Love, J. 3D printed surgical instruments: The design and fabrication process. *World J. Surg.* **2017**, *41*, 314–319. [\[CrossRef\]](#)
11. Trenfield, S.J.; Awad, A.; Goyanes, A.; Gaisford, S.; Basit, A.W. 3D printing pharmaceuticals: Drug development to frontline care. *Trends Pharmacol. Sci.* **2018**, *39*, 440–451. [\[CrossRef\]](#)
12. Murphy, S.V.; Atala, A. 3D bioprinting of tissues and organs. *Nat. Biotechnol.* **2014**, *32*, 773–785. [\[CrossRef\]](#) [\[PubMed\]](#)
13. Berglund, G.; Wisniowiecki, A.; Gawedzinski, J.; Applegate, B.; Tkaczyk, T.S. Additive manufacturing for the development of optical/photonics systems and components. *Optica* **2022**, *9*, 623–638. [\[CrossRef\]](#)
14. Ayyildiz, O. Customised spectacles using 3-D printing technology. *Clin. Exp. Optom.* **2018**, *101*, 747–751. [\[CrossRef\]](#) [\[PubMed\]](#)
15. Tsegay, F.; Ghannam, R.; Daniel, N.; Butt, H. 3D Printing Smart Eyeglass Frames: A Review. *ACS Appl. Eng. Mater.* **2023**, *1*, 1142–1163. [\[CrossRef\]](#)
16. Lee, L.; Burnett, A.M.; Panos, J.G.; Paudel, P.; Keys, D.; Ansari, H.M.; Yu, M. 3-D printed spectacles: Potential, challenges and the future. *Clin. Exp. Optom* **2020**, *103*, 590–596. [\[CrossRef\]](#) [\[PubMed\]](#)
17. Solaimani, S.; Parandian, A.; Nabiollahi, N. A holistic view on sustainability in additive and subtractive manufacturing: A comparative empirical study of eyewear production systems. *Sustainability* **2021**, *13*, 10775. [\[CrossRef\]](#)
18. Zhu, Y.; Tang, T.; Zhao, S.; Joralmon, D.; Poit, Z.; Ahire, B.; Keshav, S.; Raje, A.R.; Blair, J.; Zhang, Z.; et al. Recent advancements and applications in 3D printing of functional optics. *Addit. Manuf.* **2022**, *52*, 102682. [\[CrossRef\]](#)
19. Jia, S.; Bu, Y.; Lau, D.S.A.; Lin, Z.; Sun, T.; Lu, W.W.; Lu, S.; Ruan, C.; Chan, C.H.J. Advances in 3D bioprinting technology for functional corneal reconstruction and regeneration. *Front. Bioeng. Biotechnol.* **2022**, *10*, 1065460. [\[CrossRef\]](#)

20. Wang, Y.; Wang, J.; Ji, Z.; Yan, W.; Zhao, H.; Huang, W.; Liu, H. Application of bioprinting in ophthalmology. *Int. J. Bioprinting* **2022**, *8*, 552. [[CrossRef](#)]
21. Ruiz-Alonso, S.; Villate-Beitia, I.; Gallego, I.; Lafuente-Merchan, M.; Puras, G.; Saenz-del-Burgo, L.; Pedraz, J.L. Current insights into 3D bioprinting: An advanced approach for eye tissue regeneration. *Pharmaceutics* **2021**, *13*, 308. [[CrossRef](#)]
22. Kafle, A.; Luis, E.; Silwal, R.; Pan, H.M.; Shrestha, P.L.; Bastola, A.K. 3D/4D Printing of polymers: Fused deposition modelling (FDM), selective laser sintering (SLS), and stereolithography (SLA). *Polymers* **2021**, *13*, 3101.
23. Szabó, B.; Babuška, I. *Finite Element Analysis: Method, Verification and Validation*, 2nd ed.; Wiley: New York, NY, USA, 2021.
24. David Müzel, S.; Bonhin, E.P.; Guimarães, N.M.; Guidi, E.S. Application of the finite element method in the analysis of composite materials: A review. *Polymers* **2020**, *12*, 818. [[CrossRef](#)] [[PubMed](#)]
25. Bathe, K.J.; Zhang, H.; Ji, S. Finite element analysis of fluid flows fully coupled with structural interactions. *Comput. Struct.* **1999**, *72*, 1–16. [[CrossRef](#)]
26. Liu, X.F.; Wang, Y.; Liu, W.H. Finite element analysis of thermo-mechanical conditions inside the piston of a diesel engine. *Appl. Therm. Eng.* **2017**, *119*, 312–318. [[CrossRef](#)]
27. Rajanna, M.R.; Johnson, E.L.; Codoni, D.; Korobenko, A.; Bazilevs, Y.; Liu, N.; Lua, J.; Phan, N.; Hsu, M.C. Finite element methodology for modeling aircraft aerodynamics: Development, simulation, and validation. *Comput. Mech.* **2022**, *70*, 549–563. [[CrossRef](#)]
28. Bradai, S.; Naifar, S.; Kanoun, O. Finite element analysis of combined magnetoelectric-electrodynamic vibration energy converter. *J. Phys. Conf. Ser.* **2015**, *660*, 012111. [[CrossRef](#)]
29. Wang, T.; Green, R.; Guldiken, R.; Wang, J.; Mohapatra, S.; Mohapatra, S.S. Finite element analysis for surface acoustic wave device characteristic properties and sensitivity. *Sensors* **2019**, *19*, 1749. [[CrossRef](#)]
30. Abueidda, D.W.; Elhebeary, M.; Shiang, C.S.A.; Pang, S.; Al-Rub, R.K.A.; Jasiuk, I.M. Mechanical properties of 3D printed polymeric Gyroid cellular structures: Experimental and finite element study. *Mater. Des.* **2019**, *165*, 107597. [[CrossRef](#)]
31. Castaldo, P.; Gino, D.; Mancini, G. Safety formats for non-linear finite element analysis of reinforced concrete structures: Discussion, comparison and proposals. *Eng. Struct.* **2019**, *193*, 136–153. [[CrossRef](#)]
32. Nurhaniza, M.; Ariffin, M.K.A.; Ali, A.; Mustapha, F.; Noraini, A.W. Finite element analysis of composites materials for aerospace applications. *IOP Conf. Ser. Mater. Sci. Eng.* **2010**, *11*, 012010. [[CrossRef](#)]
33. Purohit, R.; Khitoliya, P.; Koli, D.K. Design and finite element analysis of an automotive clutch assembly. *Procedia Mater. Sci.* **2014**, *6*, 490–502. [[CrossRef](#)]
34. Soro, N.; Brassart, L.; Chen, Y.; Veidt, M.; Attar, H.; Dargusch, M.S. Finite element analysis of porous commercially pure titanium for biomedical implant application. *Mater. Sci. Eng. A* **2018**, *725*, 43–50. [[CrossRef](#)]
35. Cicciù, M. Bioengineering methods of analysis and medical devices: A current trends and state of the art. *Materials* **2020**, *13*, 797. [[CrossRef](#)] [[PubMed](#)]
36. Ramasubramanian, V.S.; Meenatchi Sundaram, S.; Thomas, R.; Ramesh, S.V.; Raghuvir Pai, B.; Hazarika, M.; Abdul Khader, S.M.; Poojary, R.G.; Girish, H.; Crasto, V.S. Finite element analysis of cornea and lid wiper during blink, with and without contact lens. *J. Ophthalmol.* **2022**, *2022*, 7930334. [[CrossRef](#)] [[PubMed](#)]
37. Moraru, E. Research on the Realization of Dental Prostheses by Selective Laser Deposition and Other Additive Technologies. Ph.D. Thesis, Politehnica University of Bucharest, Bucharest, Romania, 2021. (In Romanian).
38. Besnea, D.; Rizescu, C.I.; Rizescu, D.; Comeaga, D.; Ciobanu, R.; Moraru, E. Study of deflection behaviour of 3D printed leaf springs. In Proceedings of the 8th International Conference on Advanced Concepts in Mechanical Engineering, Iasi, Romania, 7–8 June 2018; Volume 444, p. 042008.
39. Mohamed, O.A.; Masood, S.H.; Bhowmik, J.L. Optimization of fused deposition modeling process parameters: A review of current research and future prospects. *Adv. Manuf.* **2015**, *3*, 42–53.
40. Solomon, I.J.; Sevel, P.; Gunasekaran, J. A review on the various processing parameters in FDM. *Mater. Today Proc.* **2021**, *37*, 509–514.
41. Dey, A.; Yodo, N. A systematic survey of FDM process parameter optimization and their influence on part characteristics. *J. Manuf. Mater. Process.* **2019**, *3*, 64.
42. Enemuoh, E.U.; Duginski, S.; Feyen, C.; Menta, V.G. Effect of process parameters on energy consumption, physical, and mechanical properties of fused deposition modeling. *Polymers* **2021**, *13*, 2406

Disclaimer/Publisher’s Note: The statements, opinions and data contained in all publications are solely those of the individual author(s) and contributor(s) and not of MDPI and/or the editor(s). MDPI and/or the editor(s) disclaim responsibility for any injury to people or property resulting from any ideas, methods, instructions or products referred to in the content.